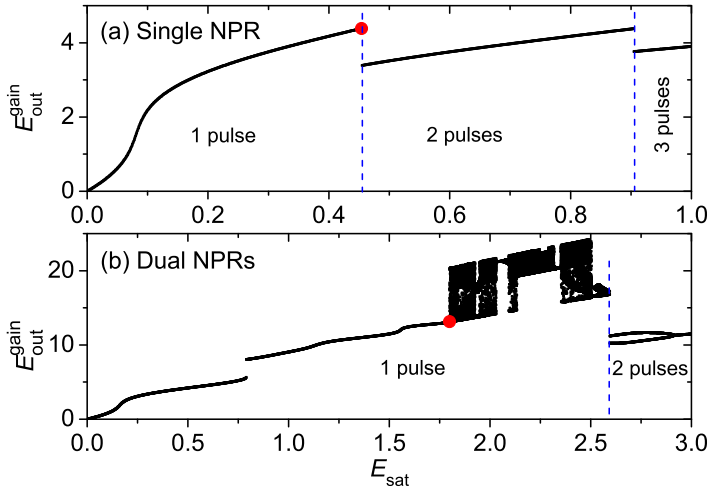

Fig. 4. The pulse energy per pulse with the increase of E_{sat}. The upper panel (a) is for the cavity with a single transmission function for generating nonlinear polarization rotation (NPR), and the bottom panel is for dual NPRs. The cavity parameters are the same as those used in Fig. 3. With a single NPR, the pulse energy will trigger the multi-pulse transition (red dot) at energy of approximately 4. The dual NPR cavity remains stable (red dot) up to an energy of approximately 13 before generating chaotic solutions. Thus the dual transmission can enhance the pulse energy by a factor of three. The blue vertical dash lines indicate the multi-pulse transition points.

defined by Eqs. (1), (3) and (4). The first cross point (red point) of the blue nonlinear loss curve and the threshold line is extended far from the first period of the nonlinear loss. Multi-pulsing can be suppressed in this broad region before the red point. We should note that bifurcation and chaos still can occur in this broad region while the loss curve has large slope [13].

Figure 4 demonstrates the simulation results with the iterative process outlined in Li *et al.* [13] for two key cases: a single transmission curve, i.e. only one set of waveplates and polarizers for generating nonlinear polarization rotation, and the dual transmission curve of Fig. 3 as illustrated in Fig. 1(b). Figure 4(b) clearly demonstrates that the multi-pulsing instability is suppressed by the proper engineering of the dual transmission curve. Indeed, a nearly 200% increase in performance can be achieved before the onset of chaotic dynamics. Given the tremendously large parameter space afforded by practical experiments, it is anticipated that this performance enhancement can be further increased. In contrast, Fig. 4(a) shows that a single transmission curve quickly trigger the multi-pulsing once the single pulse energy reaches the MPI threshold point defined by the red points in Fig. 2(a) and Fig. 3(a). To understand this enhancement more clearly, we can interpret its results by a specific example. Assume that: (i) the pulse shape (width) is not significantly altered per round trip so that the output pulse width is approximately 100fs; (ii) The cavity length is assumed to be composed of 20m of optical fiber with a nonlinearity coefficient of $2\mathrm{W}^{-1}\mathrm{km}^{-1}$; and (iii) The doped fiber will provide small signal gain 30dB. Then the laser pulse output will be limited to 33nJ while the peak power is 330W before triggering the multi-pulsing instability. After we insert the second NPR set, this energy limitation can be enhanced to about 100nJ with 200% improvement.

The simple geometrical arguments and theory expounded here build upon previous findings [13] by suggesting a practical way of generating a nonlinear transmission curve capable of

suppressing MPI. Indeed, the dual transmission is a simple and elegant way of engineering the requisite transmission. In the next section, full cavity simulations demonstrate that the simple engineering principle of transmission curve design indeed produces performance enhancement.

4. Full laser cavity dynamics with dual transmission

The simulations with the geometrical model in Section 3 has shown promising enhancement to the pulse energy with another set of NPR in the laser cavity. The simulations are based on such a generic geometrical model which can be applied in most types of mode locked laser but loss some important features of specific fiber laser cavities such as dispersion and nonlinearity. The results from the geometrical model can only show the qualitative results to demonstrate the working principle of the enhancement by the additional NPR. But since the performance of such fiber laser systems can be affected by the neglected features significantly, it's necessary to perform full simulations with a sophisticate model for such cavities. To affirm the theoretical predictions of the simplified model of the previous section, full simulations of the laser cavity shown in Fig. 1(a) are performed. The governing equations in the j-th fiber section are given by coupled nonlinear Schrödinger equations (CNLS) [12, 23, 24]:

$$i\frac{\partial u}{\partial z}+\frac{D_j}{2}\frac{\partial^2 u}{\partial t^2}-K_j u+\left(|u|^2+A|v|^2\right)u+Bv^2u^*=iR_j u\,, \tag{5a}$$

$$i\frac{\partial v}{\partial z}+\frac{D_j}{2}\frac{\partial^2 v}{\partial t^2}+K_j v+\left(|v|^2+A|u|^2\right)v+Bu^2v^*=iR_j v\,, \tag{5b}$$

where

$$R_j=\frac{2g_{0,j}}{1+\left(\|u\|^2+\|v\|^2\right)/e_{0,j}}\left(1+\tau_j\frac{\partial^2}{\partial t^2}\right)-\Gamma_j\,. \tag{6}$$

In the above system, u and v represent the two orthogonally polarized electric field envelopes in an optical fiber with birefringence K_j. The z coordinate denotes the propagating distance normalized by the length of the first fiber section, and t denotes the retarded time normalized by the full-width at half-maximum of the pulse. D_j is the averaged group velocity dispersion of the j-th fiber section (doped and undoped fiber sections), and is positive for anomalous dispersion and negative for normal dispersion. In the ANDi laser which we consider in this paper, D is always negative [9]. The nonlinear coupling parameters A (cross-phase modulations) and B (four-wave mixing) are determined by the material of the optical fiber. In axial symmetrical fibers, $A+B=1$ will be satisfied and, specific values $A=2/3$ and $B=1/3$ [23,24] are adopted in normal single mode fibers. The dissipative terms, R_j, accounting for the saturable, bandwidth limited saturating gain and attenuation, In particular, $g_{0,j}$ and $e_{0,j}$ are the nondimensional pumping strength and the saturating energy of the gain respectively for each section of fiber. The parameter τ_j characterizes the bandwidth of the pump, and Γ_j measures the distributed losses caused by the output coupling and the fiber attenuation. Note that $\|u\|^2=\int|u|^2dt$ and $\|v\|^2=\int|v|^2dt$ denote the energy in each of the orthogonally polarized electric field components where integration is for $t\in[-\infty,\infty]$.

The effect of the waveplates and passive polarizer can be modeled by the corresponding Jones matrices [12, 25]. The standard Jones matrices of the quarter-waveplate, half-waveplate and polarizer are given, respectively, by

$$W_{\frac{\lambda}{4}}=\begin{pmatrix} e^{-i\pi/4} & 0\\ 0 & e^{i\pi/4}\end{pmatrix}\,, \tag{7a}$$

$$W_{\frac{\lambda}{2}}=\begin{pmatrix} -i & 0\\ 0 & i\end{pmatrix}\,, \tag{7b}$$

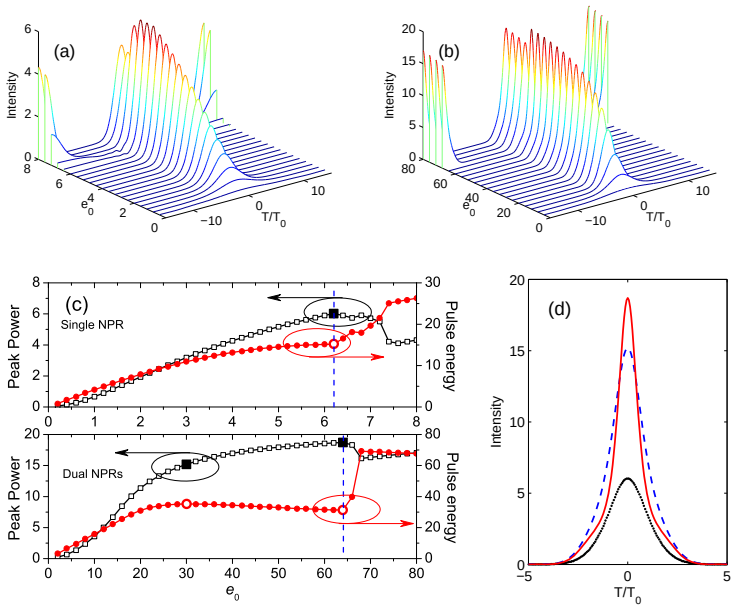

Fig. 5. The stable mode-locked pulse shape is shown as a function of increasing saturation energy $e_{0,j}$ in (a) for a single NPR laser cavity and (b) for a dual NPRs laser cavity. Panel (c) shows the pulse peak power and energy variation with $e_{0,j}$ for both lasers. The vertical blue lines indicate the multi-pulsing transition threshold. In the top panel of (c), the line with square marks shows the peak power and the line with circle marks shows the pulse energy. The zoomed solid square and hollow circle at $e_{0,1} = 6.2$ indicate the maximum peak power and pulse energy that can be obtained in this laser. There are two pair of zoomed marks in the bottom panel of (c). The left pair marks at $e_{0,1} = 30$ show the pulse with maximum pulse energy and the right pair marks at $e_{0,1} = 64$ show the pulse with maximum peak power. The three pulses indicated by the three pair zoomed marks are shown in (d). The black dot line shows the pulse with maximum energy and peak power obtained in single NPR system shown in (a) and the top panel of (c). The blue dash line/red solid line shows the pulse with maximum energy/peak power in dual NPR system shown in (b) and the bottom panel of (c). The parameters of the single NPR system are $\alpha_1 = 0$, $\alpha = 0.49\pi$, $\alpha = 0.2\pi$, $\alpha_p = 0.45\pi$, $K_1 = 0.1$, $D_1 = -0.4$, $\tau_1 = 0.1$, $\Gamma_1 = 0.1$, $g_{0,1} = 1.73$ and $e_{0,1}$ is varied. The parameters in the dual NPR system are same as the single NPR system only except that the variables $g_{0,2} = 0$ and $e_{0,2} = 0$, which means the second NPR set is passive. Other parameters of the second set NPR are same to the first set.

$$W_p = \begin{pmatrix} 1 & 0 \\ 0 & 0 \end{pmatrix} . \tag{7c}$$

These matrices are valid only when the principle axes of the devices are aligned with the fast axis of the fiber. For arbitrary orientation α_j ($j = 1,2,3,p$) shown in Fig. 1, the matrices are modified according to

$$J_j = R(\alpha_j) W R(-\alpha_j) , \tag{8}$$

where W is the Jones matrix of the device given in Eq. (7) and R is the rotation matrix

$$R(\alpha_j) = \begin{pmatrix} \cos\alpha_j & -\sin\alpha_j \\ \sin\alpha_j & \cos\alpha_j \end{pmatrix} . \tag{9}$$

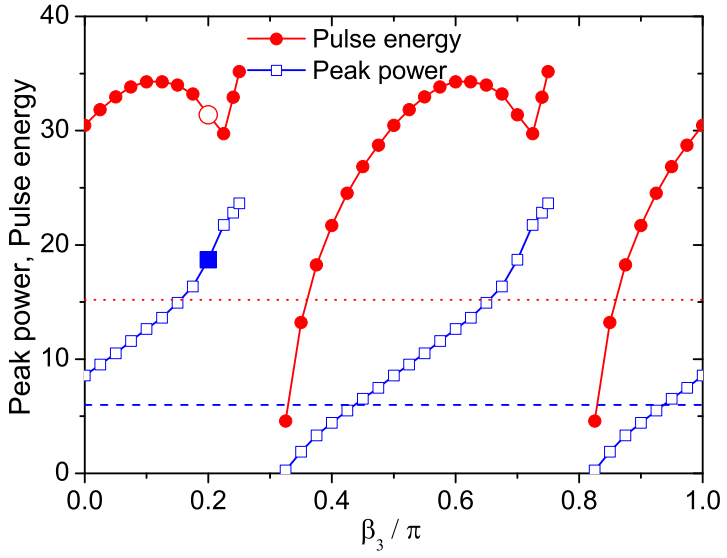

Fig. 6. The peak power (blue line with square marks) and pulse energy (red line with circle marks) with the maximum $e_{0,1}$ without triggering the multipulsing at different β_3 in dual NPRs cavity. The red dot line and blue dash line are the maximum pulse energy and peak power can be obtained in single NPR cavity. The zoomed blue square and red circle marks correspond to the results with dual NPRs in Fig. 5.

The governing evolution equations (5) together with Jones matrices (8) gives a full description of pulse propagation in the laser system. The principle of operation involves iterations of solving the CNLS over one round trip and applying the Jones matrices of the waveplates and polarizer consecutively. The discrete application of Jones matrices after each cavity round trip acts like a filter that can be tuned to control the mode-locking behavior. Indeed, they are responsible for generating the nonlinear transmission functions T_1 and T_2. Depending on their orientations, the waveplates and the polarizer can either destabilize the field propagating in the cavity or lock it into a particular polarization component so that robust mode-locking can be achieved.

Simulations of the full cavity dynamics and mode-locking for normal dispersion are shown in Fig. 5 for both a single and dual transmission configuration. In both cases stable mode-locking is achieved. However, the maximum performance using two sets of waveplates and polarizers gives a significant increase in energy delivery. In simulations, we first find a stable mode locking setting of the wavepaltes and polarizer. Then we increase the saturation energy of the gain $e_{0,1}$ slightly. The pulse peak power and energy will both increase till the multipulsing been triggered with $e_{0,1} > 6.2$. The maximum pulse peak power and energy can be obtained with these parameters are 6.0 and 15.2 as shown in Fig. 5(a). Then we add one more set of fiber, waveplates and polarizer into the cavity. The second set parameters are same to the first set shown in Fig. 5(a) except $g_{0,2} = 0$. Then $e_{0,1}$ is varied again as shown in Fig. 5(b). With the dual NPRs setting, the peak power and pulse energy can be enhanced to 18.7 and 31.4 before the multipulsing been triggered while $e_{0,1} > 64$. The peak power and pulse energy variation with the increase of $e_{0,1}$ in both cavity settings are shown in Fig. 5(c). Note that with dual NPRs

in the cavity, the maximum pulse energy 35.2 is obtained at $e_{0,1} = 30$ which is not the point with maximum peak power. The pulse waveforms with maximum peak power or energy in both settings are shown in Fig. 5(d). The significant peak power and pulse energy enhancement found in this sophistic model is consistent with the discrete, geometrical model of the last section.

To understand how to achieve maximal performance as a function of one of the parameters, a simple parameter space sweep is performed. Given the overwhelmingly large parameter space represented by the waveplates and polarizers, we will focus on this one parameter sweep in order to illustrate the dual transmission concept. Figure 6 performs a sweep of the parameter through varying the values of β_3 from 0 to π. This one parameter sweep of a dual transmission laser cavity illustrates the peak power and pulse energy with the maximum $e_{0,1}$ without triggering the multipulsing at different β_3. Note that the pulse energy shown in the figure are not always the maximum value that can be obtained with the given β_3 value. This is already known from Fig. 5(c). The maximum peak power and pulse energy from single NPR cavity is also drawn on the Figure for comparison. Note that while β_3 is tuned to about 0.3π or 0.8π, stable solution can not be obtained. It is obvious that the second set of NPR can enhance the pulse energy and peak power in most region of β_3.

5. Conclusions

Modeling and simulation are powerful tools in helping design next generation fiber lasers. It is through theoretical studies that we can suggest concrete techniques for suppressing the ubiquitous MPI limitations and potentially increase pulse energies a final order of magnitude in order to compete directly with solid state lasers. Indeed, it is a clear goal of the fiber laser community to surpass solid state performance in this current decade. Here, a simple yet effective technique is demonstrated for enhancing mode-locked energy delivery, namely a second set of waveplates and polarizer are applied to the cavity with the desired second transmission curve capable of suppressing MPI. Although the results are far from the desired order-or-magnitude increase, it does suggest a clear method by which MPI and pulse energies can be easily increased. By varying only a single parameter, an increase of 100% was easily achieved.

In ongoing investigations, it is our intent to use these simple design principles to design and engineer transmission functions capable of much larger energy enhancements. One of the primary difficulties in the theoretical modeling is the effort required to connect the desired transmission curves T_1 and T_2 (each of which has a few degrees of freedom describing its period, modulation depth, and offset) to the full cavity model and its large parameter space determined by the waveplates ($\alpha_1, \alpha_2, \alpha_3, \beta_1, \beta_2$ and β_3), the polarizers α_p and β_p, the fiber lengths (L_1 and L_2), the fast–slow axis alignments, and birefringence K_1 and K_2. This requires the engineering and nonlinear mapping of a 14-dimensional parameter space to generate the desired transmission curve $T(E)$ that has a periodic structure and whose troughs remain above the small signal gain limit [13]. Although at first such a large parameter sweep seems rather daunting, it also suggests that there is a great deal of flexibility in engineering almost any periodic transmission curve desired, thus potentially allowing for upwards of an order of magnitude increase in energy if mode-locking can be achieved on the third, fourth or higher period of the periodic transmission window.

Acknowledgments

P. K. A. Wai and Feng Li acknowledge the support of the Research Grant Council of the Hong Kong Special Administrative Region, China (project PolyU5282/11E). J. N. Kutz acknowledges support from the National Science Foundation (NSF) (DMS-1007621) and the U.S. Air Force Office of Scientific Research (AFOSR) (FA9550-09-0174).